

MICROCOPY RESOLUTION TEST CHART
NATIONAL BUREAU OF STANDARDS-1963-A

2

The Use of Electron Beam Position Modulation in Auger Depth Profile Analysis

M. S. LEUNG and G. W. STUPIAN
Chemistry and Physics Laboratory
The Aerospace Corporation
El Segundo, CA 90245

1 September 1985

DTIC
ELECTE
OCT 2 1985
S B D

APPROVED FOR PUBLIC RELEASE;
DISTRIBUTION UNLIMITED

AD-A159 712

DTIC FILE COPY

Prepared for
SPACE DIVISION
AIR FORCE SYSTEMS COMMAND
Los Angeles Air Force Station
P.O. Box 92960, Worldway Postal Center
Los Angeles, CA 90009-2960

85 10 02 006

This report was submitted by The Aerospace Corporation, El Segundo, CA 90245, under Contract No. F04701-83-C-0084 with the Space Division, P.O. Box 92960, Worldway Postal Center, Los Angeles, CA 90009. It was reviewed and approved for The Aerospace Corporation by S. Feuerstein, Director, Chemistry and Physics Laboratory.

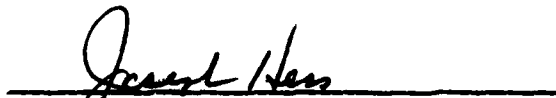
Lt Carl Baner, SD/CGX, was the project officer for the Mission-Oriented Investigation and Experimentation (MOIE) Program.

This report has been reviewed by the Public Affairs Office (PAS) and is releasable to the National Technical Information Service (NTIS). At NTIS, it will be available to the general public, including foreign nationals.

This technical report has been reviewed and is approved for publication. Publication of this report does not constitute Air Force approval of the report's findings or conclusions. It is published only for the exchange and stimulation of ideas.



CARL BANER, Lt, USAF
MOIE Project Officer
SD/CGX



JOSEPH HESS, GM-15
Director, AFSTC West Coast Office
AFSTC/WCO OL-AB

UNCLASSIFIED

SECURITY CLASSIFICATION OF THIS PAGE (When Data Entered)

REPORT DOCUMENTATION PAGE		READ INSTRUCTIONS BEFORE COMPLETING FORM
1. REPORT NUMBER TR-85-60	2. GOVT ACCESSION NO. AD-A159 712	3. RECIPIENT'S CATALOG NUMBER
4. TITLE (and Subtitle) THE USE OF ELECTRON BEAM POSITION MODULATION IN AUGER DEPTH PROFILE ANALYSIS	7. AUTHOR(s) Martin S. Leung and Gary W. Stupian	5. TYPE OF REPORT & PERIOD COVERED
		6. PERFORMING ORG. REPORT NUMBER TR-0084A(5945-02)-2
9. PERFORMING ORGANIZATION NAME AND ADDRESS The Aerospace Corporation El Segundo, Calif. 90245	8. CONTRACT OR GRANT NUMBER(s) F04701-83-C-0084	
11. CONTROLLING OFFICE NAME AND ADDRESS Space Division Los Angeles Air Force Station Los Angeles, Calif. 90009-2960	10. PROGRAM ELEMENT, PROJECT, TASK AREA & WORK UNIT NUMBERS	
	12. REPORT DATE 1 September 1985	13. NUMBER OF PAGES 21
14. MONITORING AGENCY NAME & ADDRESS (if different from Controlling Office)	15. SECURITY CLASS. (of this report) Unclassified	
	15a. DECLASSIFICATION/DOWNGRADING SCHEDULE	
16. DISTRIBUTION STATEMENT (of this Report) Approved for public release; distribution unlimited.		
17. DISTRIBUTION STATEMENT (of the abstract entered in Block 20, if different from Report)		
18. SUPPLEMENTARY NOTES		
19. KEY WORDS (Continue on reverse side if necessary and identify by block number) Auger Spectroscopy Depth Profile Analysis		
20. ABSTRACT (Continue on reverse side if necessary and identify by block number) By combining Auger analysis with ion etching, the scanning Auger microprobe (SAM) provides "three-dimensional" composition information not readily obtainable from other analytical methods. As this technique is being applied to the analysis of microelectronic devices with increasingly smaller dimensions, two major limitations become evident: (1) features of interest in microelectronic circuits are often comparable in size to the beam		

SECURITY CLASSIFICATION OF THIS PAGE(When Data Entered)

18. KEY WORDS (Continued)

20. ABSTRACT (Continued)

diameter of commercial Auger microprobes, and (2) the electron beam tends to drift on the specimen surface because of mechanical instability and differential thermal expansion. Because Auger depth profiling requires relatively low sputter rates for good depth resolution, depth profiles of small features can be seriously degraded by beam drift. In this report, we describe a technique that will eliminate the error and uncertainty caused by beam instability. In our technique, the analyzing beam is scanned repetitively across the feature to be profiled, and the Auger signal is synchronously detected at the scan frequency. The resultant Auger signal magnitude is shown to be unaffected by beam drift when compared to conventional detection methods.

PREFACE

We wish to thank Dr. H. K. A. Kan and Dr. G. Eng for helpful discussions.

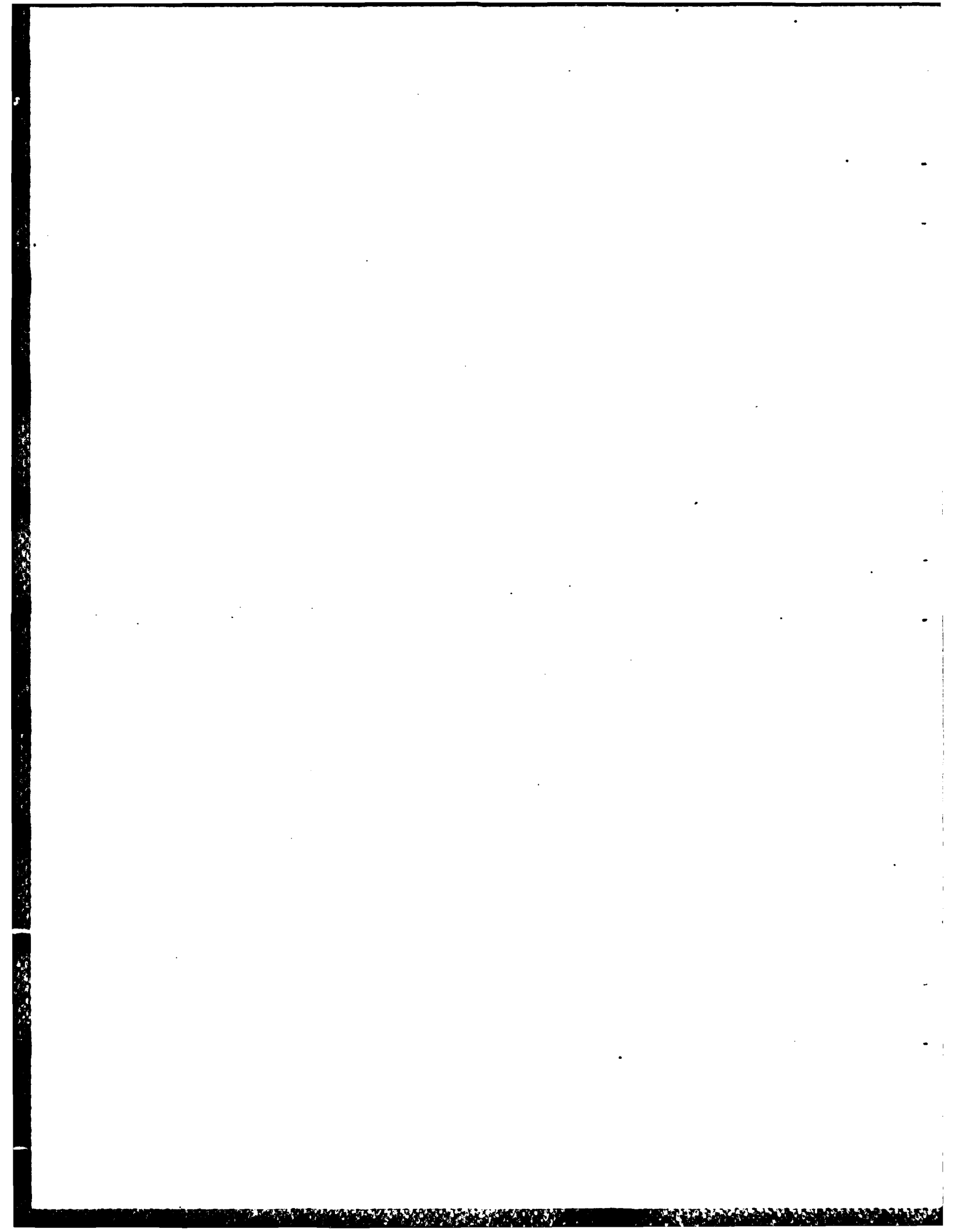
S DTIC
ELECTE **D**
OCT 2 1985
B

Accession For	
NTIS GRA&I	<input checked="" type="checkbox"/>
DTIC TAB	<input type="checkbox"/>
Unannounced	<input type="checkbox"/>
Justification	
By _____	
Distribution/	
Availability Codes	
Dist	Avail and/or Special
A-1	



CONTENTS

PREFACE.....	1
I. INTRODUCTION.....	7
II. BACKGROUND DISCUSSION.....	9
III. EXPERIMENTAL.....	13
IV. THEORETICAL CONSIDERATIONS.....	15
V. RESULTS AND DISCUSSION.....	21
VI. SUMMARY AND CONCLUSIONS.....	25



FIGURES

1.	Principles of Position Modulation.....	10
2.	Experimental Configuration of SAM for Position Modulation.....	14
3.	A Specimen Geometry of Interest: Scan of Total Length $2L$ Over a Strip of Length w , with Edge a Distance l from Start of Scan.....	16
4.	Beam Intensity as Function of Position for Square Electron Beam.....	17
5.	(a) Auger Signal Magnitude and (b) Auger Signal Phase as a Function of Position of a Gold Strip Along Scan Line.....	22
6.	Auger Depth Profile, Position Modulation, Au Metallization on GaAs.....	23

I. INTRODUCTION

The scanning Auger microprobe (SAM) provides spatially resolved elemental analyses of specimens. When combined with ion etching, elemental distribution in all three spatial dimensions can be determined. Unfortunately, the usefulness of commercial SAMs for the characterization of small features is limited by drift of the analyzing electron beam relative to the specimen as a result of mechanical and thermal instabilities in the instrument.

In this report, we describe a "position modulation" technique devised to overcome the limitation imposed on SAMs by beam instability. With the use of the position modulation method, the sensitivity of Auger signal amplitudes to beam position drift is eliminated, albeit at the expense of some reduction in signal-to-noise ratio. The theory underlying position modulation is developed, and experimental data illustrating the application of the technique are presented.

II. BACKGROUND DISCUSSION

In the conventional method of Auger depth profiling, the analyzing beam is set at a point of interest, and the peak-to-peak Auger signal amplitudes of elements are recorded as a function of time while the surface is sputtered by an ion beam. A plot of Auger signal amplitudes versus sputtering time represents elemental concentrations as a function of depth. Instability in the position of the analyzing beam is detrimental because minor movement can shift the beam away from the feature of interest. As a result, beam instability is an especially serious problem when a well-resolved composition profile of a small feature is desired. The reason is that good depth resolution requires low sputter rates, which translates to long sputtering time and consequently to more opportunity for the beam to move away from the region of interest.

The position modulation technique was developed to eliminate the error and uncertainty caused by beam instability, particularly in those situations where the magnitude of the electron beam drift is comparable to the size of the feature of interest. The principle of this technique is illustrated in Fig. 1, in which the feature of interest is a strip of element A deposited on a substrate of element B. In the position modulation technique, the analyzing electron beam is scanned repetitively across the feature of interest (Fig. 1a) to generate a secondary electron signal that is periodic. This periodic secondary electron signal contains components at the scan frequency corresponding to the Auger electrons emitted by elements present along the scan line (Figs. 1b and 1c). When detected with a lock-in amplifier (Fig. 1d), the amplitude and phase of the Auger signals of a particular feature depend on where the feature is found on the scan line. Note that the periodic signals of A and B are out of phase, and therefore their Auger signals have opposite signs. This phase information is critical for distinguishing between elements inside and outside the feature of interest. More important, it can be shown that the magnitude of the signal produced by position modulation is independent of the position of the feature and therefore is unaffected by beam drift as long as the feature stays within the scan line.

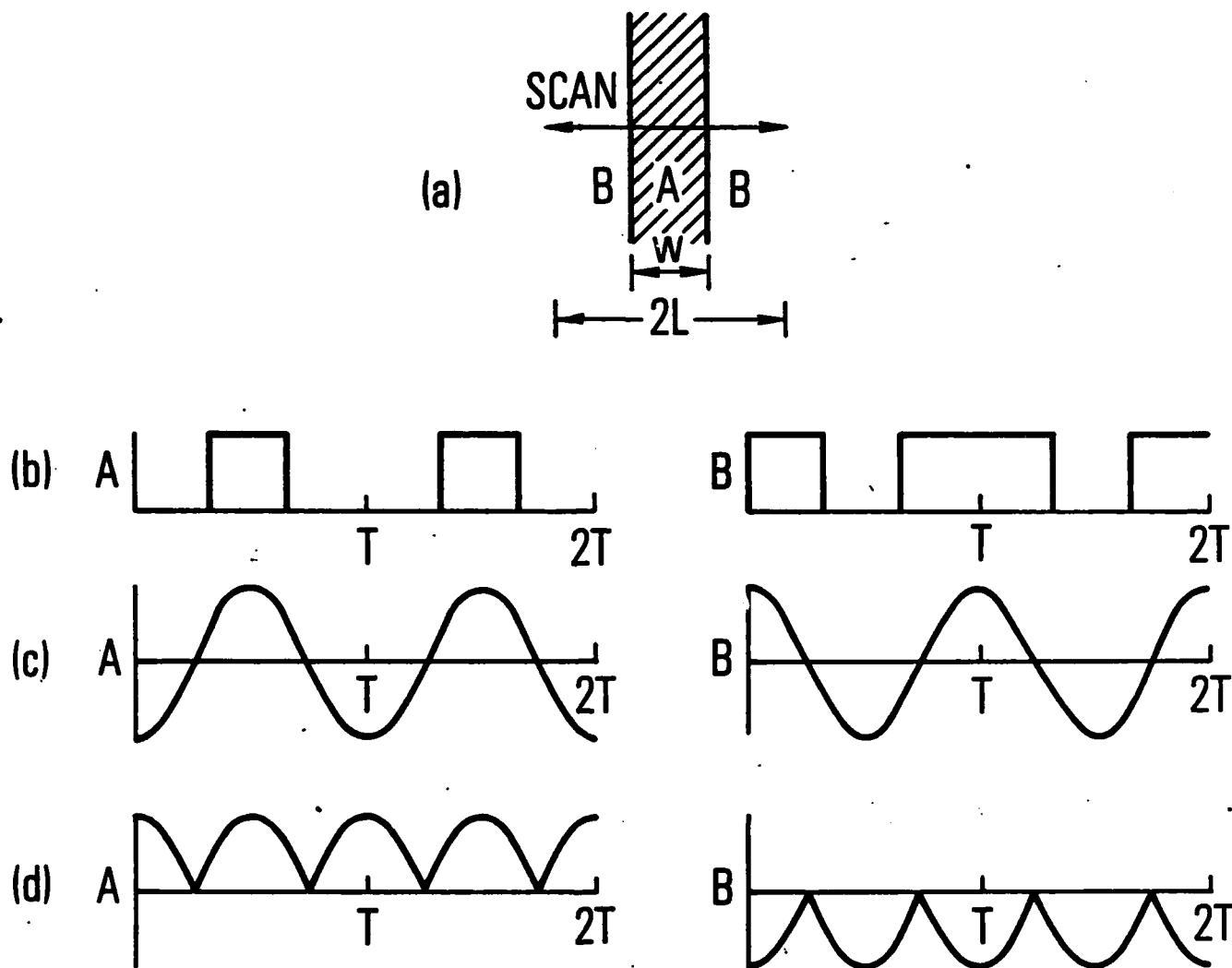


Figure 1. Principles of position modulation. (a) Analyzing electron beam scans repetitively across a feature of width w composed of element "A" on a substrate of element "B". The beam scans along a line of total length $2L$ in a time T . (b) As the spectrometer scans sequentially through electron energy regions corresponding to elements A and B, Auger signals periodic with the scan frequency are produced. (c) These periodic signals have components at the scan frequency arising from elements A and B, but with different phases corresponding to their different positions along the scan line. (d) The lock-in amplifier synchronously chops signal components at the scan frequency. With proper phase adjustment and filtering, d.c. levels corresponding to elements A and B are obtained as the spectrometer scans through the appropriate energy ranges. In the case illustrated, these signals have opposite phases.

Depth profiles are obtained by combining position modulation with ion etching, similar to the conventional Auger depth profiling method. In the situation represented in Fig. 1, a conventional Auger depth profile taken through the strip will show a decrease in the concentration of element A and the emergence of substrate element B as the strip is sputtered away. In the position-modulated depth profile, A and B will both be detected initially, but their Auger signals will have opposite signs. As the strip is sputtered away, the amplitudes of the periodic signal components of both A and B vanish, and thus the position-modulated Auger signals of both elements A and B disappear together. The interpretation of position-modulated sputter depth profiles is straightforward once the detection system is understood. An example of a position-modulated depth profile will be presented and discussed.

III. EXPERIMENTAL

The experimental configuration using the Perkin-Elmer Physical Electronics model 590 SAM for position modulation measurements is illustrated in Fig. 2. This arrangement does not differ substantially from the normal configuration, and no modification to the instrument is required. The SAM is used in the line-scan mode, and the electron beam scans repeatedly across a feature of interest. The electron energy analyzer sweeps through the energy ranges corresponding to elements to be detected. The first lock-in amplifier (LI No. 1) is a component of the Auger system that is not fundamental to the position modulation technique. LI No. 1 is used to differentiate the secondary electron spectrum with respect to energy. Differentiation reduces the large, slowly varying background that would otherwise interfere with signal amplification. In the position modulation technique, the energy-derivative Auger signal is the input to the second lock-in amplifier (LI No. 2), which derives its phase reference signal from the beam line scan. Because we want to determine "magnitudes" of Auger signals, LI No. 2 is a "quadrature" lock-in amplifier providing two synchronously detected outputs that differ as a consequence of a precise 90 deg relative phase shift in the reference signal. The magnitude of an Auger signal is defined as the square root of the sum of the squares of the quadrature outputs, whereas the signal phase is determined from their ratio.

To carry out a position-modulated depth profile, a Z80-based microcomputer system developed in our laboratory is used to control the electron energy analyzer and to collect the necessary Auger data. The computer acquires the peak-to-peak amplitudes of the Auger signal and its quadrature, stores the energies at which the signal maxima and minima occur, and keeps track of the sputtering time. Position-modulated depth profiles are computed and plotted from the stored data.

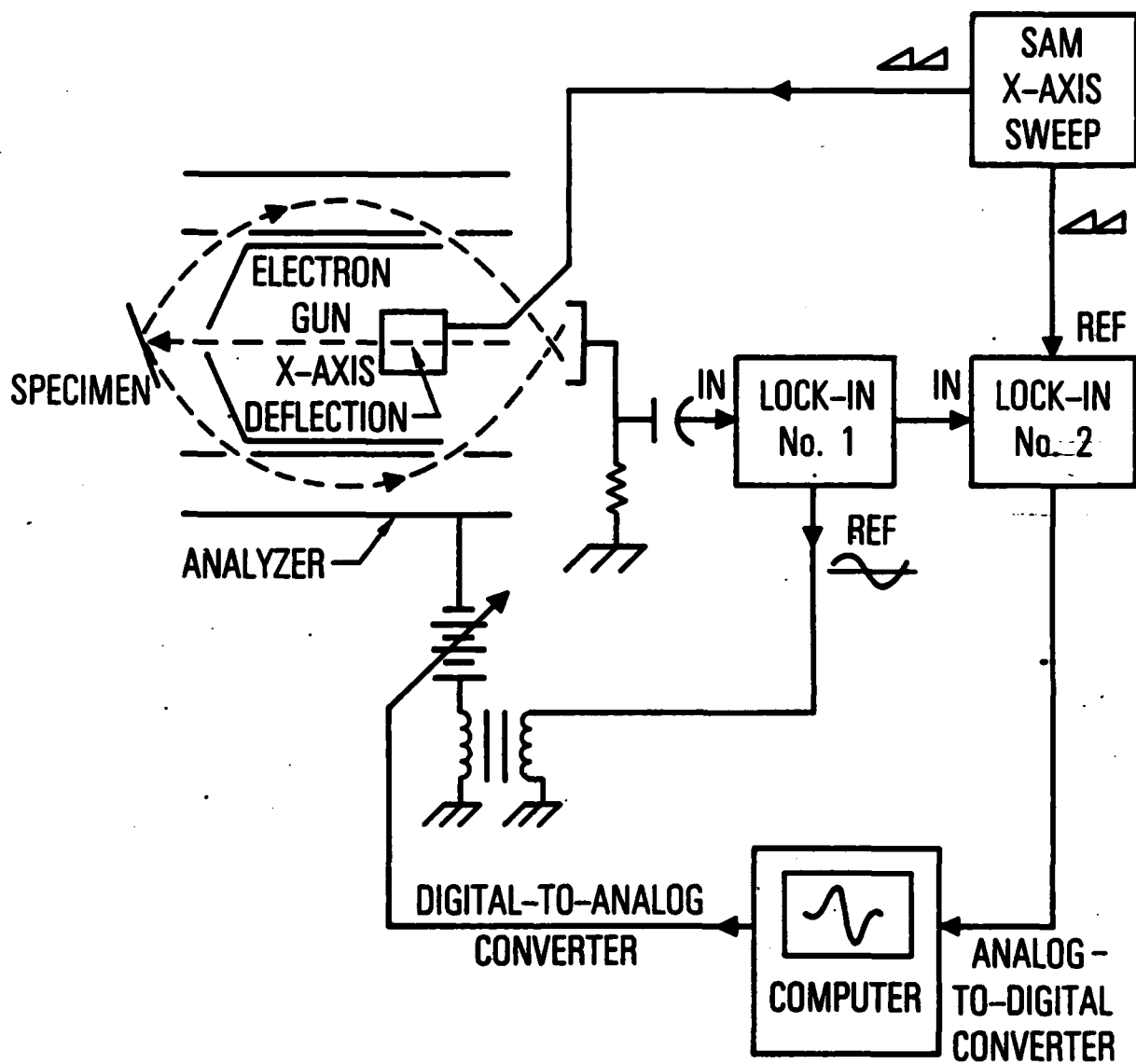


Figure 2. Experimental configuration of SAM for position modulation.

IV. THEORETICAL CONSIDERATIONS

The amplitude of an Auger signal detected using position modulation is readily derived. The result illustrates the independence of signal amplitude on movement of the electron beam. To demonstrate this property of position modulation, we shall calculate the Auger signal amplitude explicitly for the specimen geometry illustrated in Fig. 3. This geometry is well suited for application of the position modulation technique and might represent the Schottky gate metallization of a metal-semiconductor microwave field-effect transistor (FET). The feature has a width w and is taken to be homogeneous along its length and width. In the simplest experimental situation, elemental compositions are uniform both in the strip and in the region outside the strip, although the strip will in general have a layered structure. The analyzing electron beam of the SAM at the specimen surface is, for convenience, taken to be a square of uniform current density with side D to simplify the analysis. These assumptions do not affect our general conclusions.

Suppose that the electron beam, using the secondary (or absorbed current) imaging mode, is set to scan along a line of length $2L$ with the strip at its center. The parameter " l ," defined in Fig. 3 as the distance of the strip from one end of the line scan, varies as the electron beam line is moved with respect to the strip. Drift in the position of the line scan with respect to the strip corresponds to a change in l , which is completely equivalent to a change in the phase reference of LI No. 2.

Provided that the time constant of LI No. 1 is much less than the beam scan period, the output of LI No. 1 is $f(x) dn(E)/dE$, where the function $f(x)$ is sketched in Fig. 4. Because scan position varies linearly with time, we can equivalently consider the function of Fig. 4 as a function of time, denoted $f(t)$. The various distances defined in Fig. 4 can equivalently be described by the times required by the electron beam to sweep through these distances. The subsequent discussion is somewhat more natural in the time domain.

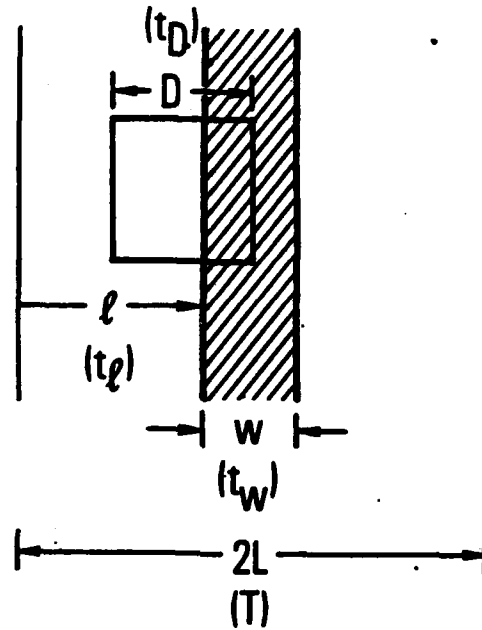


Figure 3. A specimen geometry of interest: scan of total length $2L$ over a strip of length w , with edge l from start of scan. The electron beam has uniform flux distribution over a square of side D . Scan position varies linearly with time, and instead of distances the geometry is equivalently described by the times (T , t_w , t_l , and t_D) required by the beam to scan through the characteristic distances.

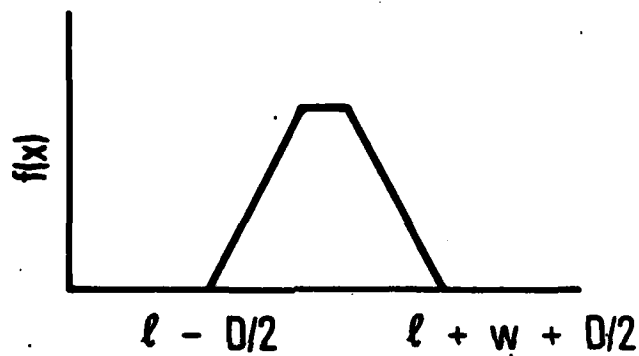


Figure 4. Beam intensity as function of position for square electron beam. Maximum amplitude of $f(x)$: 1 for $D < w$; w/D for $D > w$. (Fourier coefficients are the same for both cases.)

When the electron beam is scanned repetitively along a line across the feature of interest, $f(t)$ is a periodic function and may be represented as a Fourier series

$$f(t) = \sum_{n=0}^{\infty} [a_n \cos(2n\pi t/T) + b_n \sin(2n\pi t/T)] \quad (1)$$

The Fourier coefficients are

$$a_n = [T/(n^2 \pi^2 t_D)] \sin(n\pi t_D/T) \{ \sin[2n\pi(t_1 + t_w)/T] - \sin(2n\pi t_1/T) \} \quad (2a)$$

and

$$b_n = [T/(n^2 \pi^2 t_D)] \sin(n\pi t_D/T) \{ \cos(2n\pi t_1/L) - \cos[2n\pi(t_1 + t_w)/T] \} \quad (2b)$$

Consider now the output of LI No. 2. A lock-in amplifier may be viewed as a heterodyne mixer, which multiplies the input by a square wave with the scan period T :

$$\begin{aligned} C(t) &= -1 & 0 < t < t_r, \\ &= +1 & t_r < t < t_r + T/2, \\ &= -1 & t_r + T/2 < T. \end{aligned} \quad (3)$$

The quantity t_r is the adjustable phase shift of the lock-in amplifier. $C(t)$ may be expanded in a Fourier series as

$$C(t) = (4/\pi) \sum_{k=1}^{\infty} [1/(2k-1)] \sin[2\pi(2k-1)(t - t_r)/T] \quad (4)$$

Only odd harmonics of the scan frequency are present. The output of the mixer of the lock-in amplifier is proportional to $f(t) \cdot C(t) \cdot dn(E)/dE$. A lock-in detector of the "quadrature" type incorporates a second mixer that forms the product of $f(t) \cdot dn(E)/dE$ and a square wave shifted by 90 deg with respect to $C(t)$. The "in-phase" and "quadrature" outputs of the lock-in, denoted by S^I and S^Q , are the components of the respective mixers at zero frequency. These

outputs are obtained by filtering the mixer stage outputs, and for our particular geometry are given by the expressions

$$S^I = -[2T/(\pi^3 t_D)] \sum_{k=1}^{\infty} [1/(2k-1)^3] \sin[(2k-1)\pi t_d/T] \quad (5a)$$

$$\{\cos[2(2k-1)\pi(t_1 - t_r + t_w)/T] - \cos[2(2k-1)\pi(t_1 - t_r)/T]\} dn(E)/dE$$

and

$$S^Q = [2T/(\pi^3 t_D)] \sum_{k=1}^{\infty} (-1)^{k+1} [1/(2k-1)]^3 \sin[(2k-1)\pi t_D/T] \quad (5b)$$

$$\{\sin[2(2k-1)\pi(t_1 - t_r + t_w)/T] - \sin[2(2k-1)\pi(t_1 - t_r)/T]\} dn(E)/dE$$

We may approximate S^I and S^Q by the first terms in these series expansions, because additional terms in the series corresponding to third and higher (nth) order harmonics fall off at least as rapidly as $1/n^2$ (in the limit of a small beam diameter) for the specimen geometry under discussion. Many lock-in detectors employ tuned amplifiers ahead of the mixers and in fact directly eliminate higher terms in the series expansions of Eqs. (5a) and (5b).

The effect of the second lock-in, according to Eqs. (5a) and (5b), has been to multiply the ordinary derivative Auger signal, $dn(E)/dE$, by a geometrical factor. The quantities S^I and S^Q are taken to be the peak-to-peak amplitudes of the in-phase and quadrature Auger signals as the electron analyzer scans through the energy ranges corresponding to elements of interest. The sign of S^I or S^Q is defined as positive if the negative extremum of the derivative Auger signal occurs at higher kinetic energy than the positive extremum. We compute and store the quantities

$$\sqrt{(S^I)^2 + (S^Q)^2} = (2\sqrt{2} L/\pi^2 D) \sin(\pi D/2L) [1 - \cos(\pi w/L)]^{1/2} dn(E)/dE \quad (6a)$$

the signal magnitude, and

$$\theta = \arctan(S^I/S^Q)$$

$$\theta = (\pi/L) (1 + r + w/2) \quad (-\pi/2 < \theta < \pi/2) \quad (6b)$$

the signal phase. The distances, rather than the scan times, have again been employed in the final results of Eqs. (6a) and (6b).

Some general features of the position modulation method are apparent from Eqs. (6a) and (6b). With position modulation, Auger signals of a given element in different portions of the scan can cancel. In fact Auger signals vanish for elements present everywhere along the scan line. In the limit $w \gg \lambda$, phase differences become unimportant and the Auger signal is proportional to $(w/2L) \cdot dn(E)/dE$, just as in conventional Auger signal detection. If an element is present only outside of the strip rather than in the strip, the corresponding Auger signal amplitude is unchanged, but the phase is reversed. Consequently, the sign (phase) of the Auger signal is an indication of whether an element is inside or outside of the region of interest.

The most striking aspect of position modulation is that the Auger signal amplitudes are independent of drift in electron beam position, unless the beam scan line drifts completely off of the strip. In a typical application, when small features are to be analyzed, one often must have a beam diameter approximately equal to the feature width, i.e., $w \approx D$. Without position modulation, position drift of one beam diameter would then result in the complete loss of Auger signals from elements within the feature. With position modulation, Auger signal amplitudes will not change, according to Eq. (6a). With the use of position modulation, beam drift will result in a change in signal phase. Phase information is stored along with signal amplitude and can be employed to distinguish between elements inside and outside of the feature of interest.

V. RESULTS AND DISCUSSION

The basic concepts of position modulation were verified experimentally using a specimen geometry similar to that of Fig. 3. The analyzing electron beam was scanned across a gold strip deposited on GaAs. The length of the scan was about three times the width of the strip. The MNN gold Auger peak at 69 eV was monitored while the position of the strip relative to the scan line was changed using the micrometer adjustments of the SAM specimen stage. The Auger signal magnitude and phase, as defined in Eqs. (6a) and (6b), are shown as a function of strip position in Fig. 5. The signal magnitude is indeed independent of position, while the phase changes in agreement with Eq. (6b). The change in phase angle is indeed linear with change in strip position. The slope of the phase angle as a function of position measured from Fig. 5b is 6.5, in good agreement with the value 2π calculated from Eq. (6b). The apparent discontinuity in phase angle evident in Fig. 5b is simply a consequence of the definition of Eq. (6b).

A gold strip approximately 10 μm wide, deposited on GaAs, was profiled using position modulation. In the depth profile obtained from this specimen (Fig. 6), Auger signals of opposite relative phase have been represented by circles and by filled squares. The phase of the Auger gold signal is opposite to the phase of the gallium, arsenic, and oxygen signals. Gold is found only in the strip, while gallium and arsenic are located along the scan line outside the strip. The Auger signals all go to zero as the gold is sputtered away.

We have examined simple cases in which a given element is present only in a particular region and has a uniform composition within that region. This idealization is realistic in many situations normally encountered in the analysis of microelectronic devices.

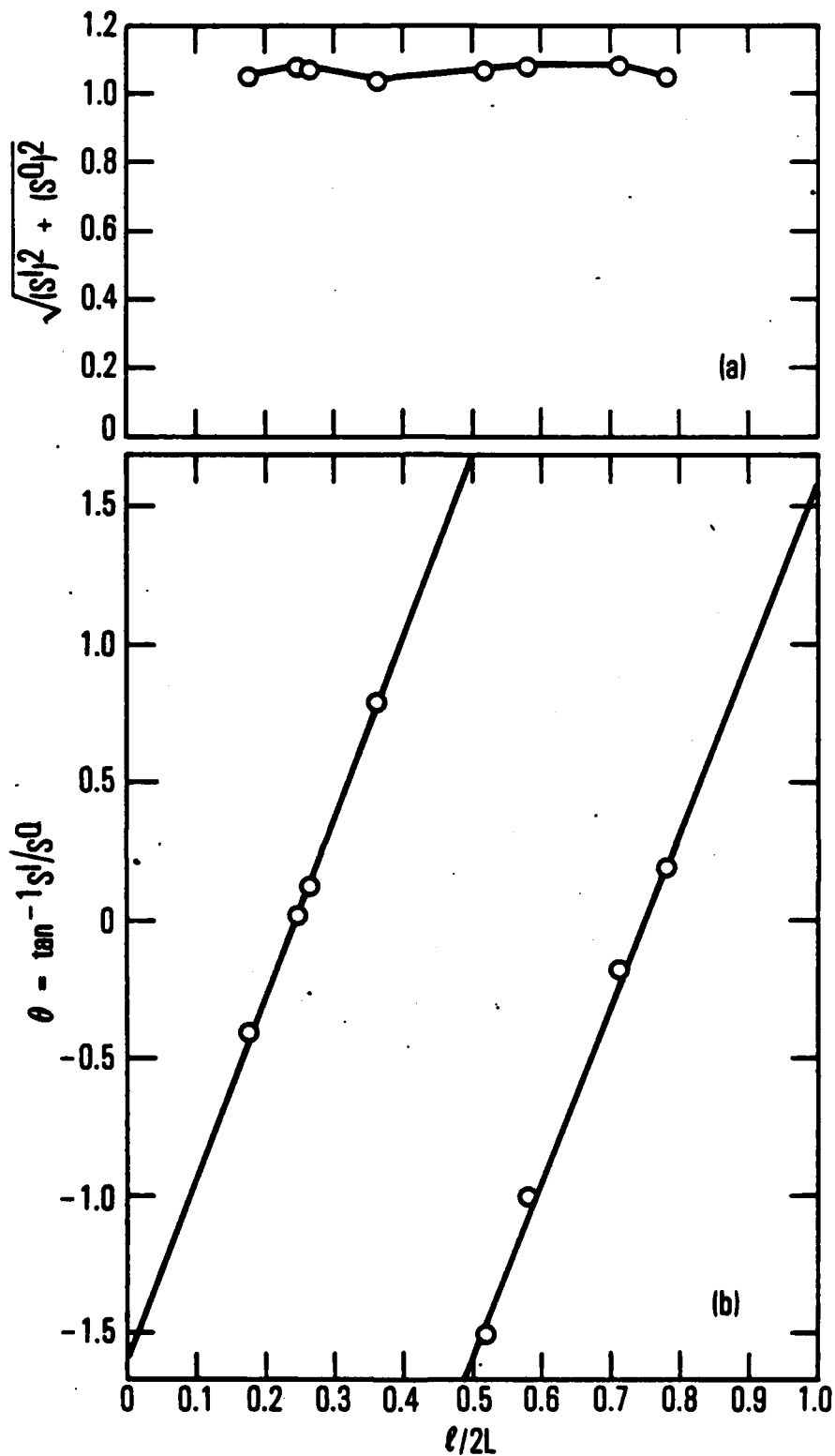


Figure 5. (a) Auger signal magnitude and (b) Auger signal phase as a function of position of a gold strip along scan line. Note that the signal magnitude is essentially independent of position.

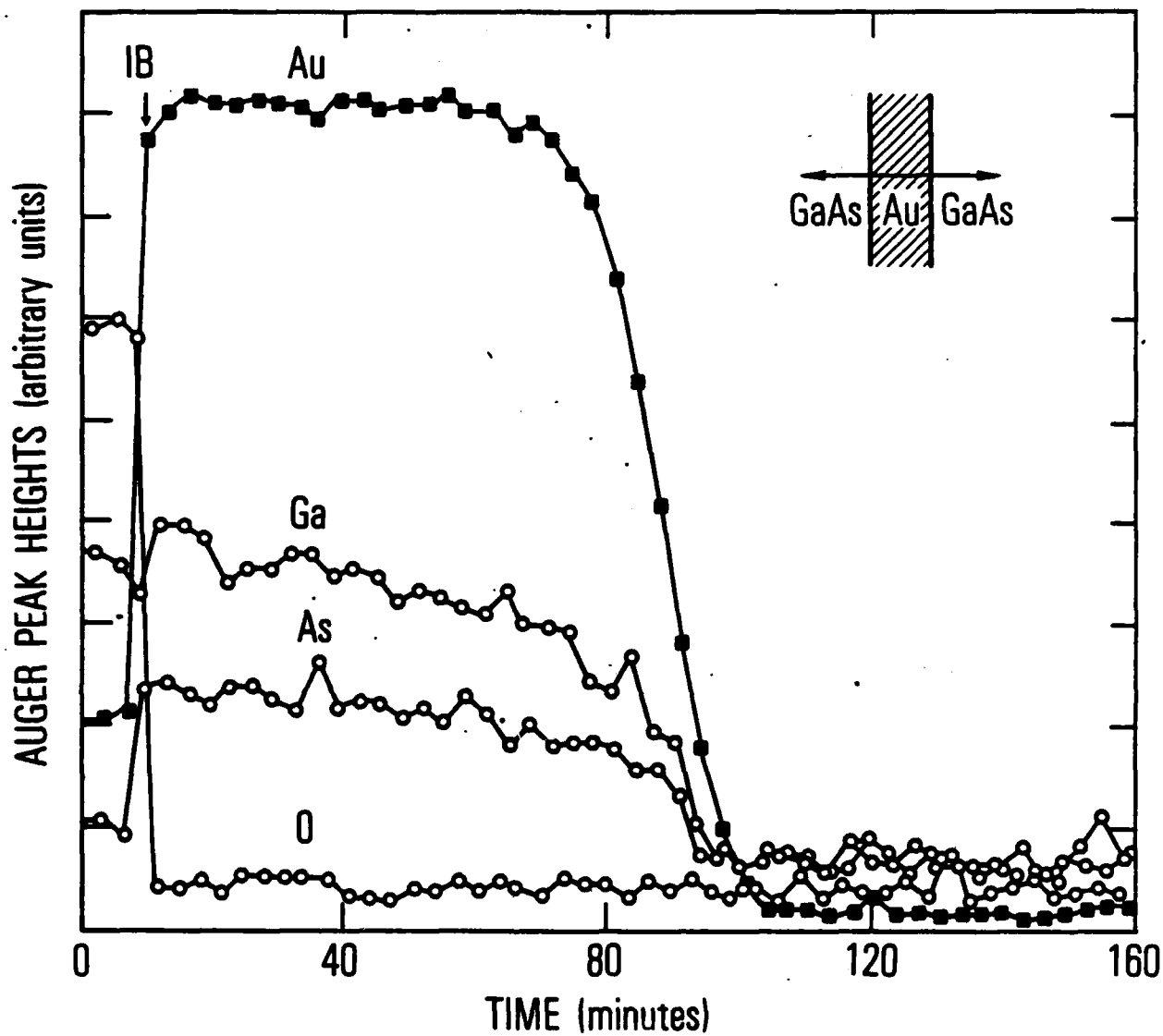


Figure 6. Auger depth profile, position modulation, Au metallization on GaAs. Auger signals of one phase (Au) plotted as filled squares, signals of opposite phase (O, Ga, As) plotted as circles. Oxygen is present only on the surface and is sputtered away very quickly. Symbol "IB" denotes time at which sputtering (in bombardment) began.

VI. SUMMARY AND CONCLUSIONS

We have demonstrated that limitations imposed by beam position instability on the Auger microprobe analysis of small features may be circumvented using position modulation for specimen geometries of practical interest. The position modulation technique permits a trade-off between signal-to-noise ratio and the sensitivity of Auger signal amplitudes to drift in spatial position of the analyzing electron beam. The advantage afforded by position modulation cannot readily be achieved by other simple tricks such as increasing the diameter of the electron beam. For example, if beam diameter is increased, elements inside and outside of the feature of interest are not distinguishable. The phase information obtained using position modulation helps resolve such ambiguities. Position modulation is particularly suited to the analysis of microelectronic devices (e.g., microwave FETs), where the dimensions of features of interest are comparable to the electron beam diameter and beam position drift found in most SAMs now in use.

LABORATORY OPERATIONS

The Laboratory Operations of The Aerospace Corporation is conducting experimental and theoretical investigations necessary for the evaluation and application of scientific advances to new military space systems. Versatility and flexibility have been developed to a high degree by the laboratory personnel in dealing with the many problems encountered in the nation's rapidly developing space systems. Expertise in the latest scientific developments is vital to the accomplishment of tasks related to these problems. The laboratories that contribute to this research are:

Aerophysics Laboratory: Launch vehicle and reentry fluid mechanics, heat transfer and flight dynamics; chemical and electric propulsion, propellant chemistry, environmental hazards, trace detection; spacecraft structural mechanics, contamination, thermal and structural control; high temperature thermomechanics, gas kinetics and radiation; cw and pulsed laser development including chemical kinetics, spectroscopy, optical resonators, beam control, atmospheric propagation, laser effects and countermeasures.

Chemistry and Physics Laboratory: Atmospheric chemical reactions, atmospheric optics, light scattering, state-specific chemical reactions and radiation transport in rocket plumes, applied laser spectroscopy, laser chemistry, laser optoelectronics, solar cell physics, battery electrochemistry, space vacuum and radiation effects on materials, lubrication and surface phenomena, thermionic emission, photosensitive materials and detectors, atomic frequency standards, and environmental chemistry.

Computer Science Laboratory: Program verification, program translation, performance-sensitive system design, distributed architectures for spaceborne computers, fault-tolerant computer systems, artificial intelligence and microelectronics applications.

Electronics Research Laboratory: Microelectronics, GaAs low noise and power devices, semiconductor lasers, electromagnetic and optical propagation phenomena, quantum electronics, laser communications, lidar, and electro-optics; communication sciences, applied electronics, semiconductor crystal and device physics, radiometric imaging; millimeter wave, microwave technology, and RF systems research.

Materials Sciences Laboratory: Development of new materials: metal matrix composites, polymers, and new forms of carbon; nondestructive evaluation, component failure analysis and reliability; fracture mechanics and stress corrosion; analysis and evaluation of materials at cryogenic and elevated temperatures as well as in space and enemy-induced environments.

Space Sciences Laboratory: Magnetospheric, auroral and cosmic ray physics, wave-particle interactions, magnetospheric plasma waves; atmospheric and ionospheric physics, density and composition of the upper atmosphere, remote sensing using atmospheric radiation; solar physics, infrared astronomy, infrared signature analysis; effects of solar activity, magnetic storms and nuclear explosions on the earth's atmosphere, ionosphere and magnetosphere; effects of electromagnetic and particulate radiations on space systems; space instrumentation.

END

FILMED

11-85

DTIC